

12-28-1995

Utilization of an Electron-Beam Tester for Determining Internal Electric Field Profiles in Micro-Structured Thin-Film Semiconductor Devices

A. Jank

University of Kaiserslautern

M. Jung

University of Kaiserslautern

M. Lambert

University of Kaiserslautern

G. Lichter

University of Kaiserslautern

H. Schmoranzer

University of Kaiserslautern, agschmor@rhrk.uni-kl.de

Follow this and additional works at: <https://digitalcommons.usu.edu/microscopy>



Part of the [Biology Commons](#)

Recommended Citation

Jank, A.; Jung, M.; Lambert, M.; Lichter, G.; and Schmoranzer, H. (1995) "Utilization of an Electron-Beam Tester for Determining Internal Electric Field Profiles in Micro-Structured Thin-Film Semiconductor Devices," *Scanning Microscopy*. Vol. 10 : No. 1 , Article 4.

Available at: <https://digitalcommons.usu.edu/microscopy/vol10/iss1/4>

This Article is brought to you for free and open access by the Western Dairy Center at DigitalCommons@USU. It has been accepted for inclusion in Scanning Microscopy by an authorized administrator of DigitalCommons@USU. For more information, please contact digitalcommons@usu.edu.



UTILIZATION OF AN ELECTRON-BEAM TESTER FOR DETERMINING INTERNAL ELECTRIC FIELD PROFILES IN MICRO-STRUCTURED THIN-FILM SEMICONDUCTOR DEVICES

A. Jank, M. Jung, M. Lambert, G. Lichter and H. Schmoranzer*

Department of Physics, University of Kaiserslautern, D-67663 Kaiserslautern, Germany

(Received for publication June 15, 1995 and in revised form December 28, 1995)

Abstract

An electron-beam tester was used to determine the depth profile of the internal potential distribution in an a-Si:H solar cell and hence the internal electric field profile. The a-Si:H solar cells were prepared for the measurements with the electron-beam tester by low-energy chemical plasma beam etching through a plasma-resistant mask structured by electron-beam lithography. In contrast to an earlier work, the solar cells were *in situ* illuminated and the electric field profiles were determined for new, degraded and *in situ* annealed solar cells at various cell temperatures. The measuring results demonstrate that the electron-beam testing technique in combination with a suitable micro-structure preparation method is appropriate to measure internal electric field profiles in semiconductor devices as, e.g., solar cells for arbitrarily chosen bias and illumination states.

Key Words: Depth distribution of potential, internal electric field, thin film semiconductor device, amorphous silicon solar cell, potential contrast, electron-beam tester, electron-beam lithography, micro-structuring, plasma-beam etching.

Introduction

The profile of the electric field in the intrinsic region of a-Si:H solar cells essentially determines the collection efficiency and thus the conversion efficiency of these devices. With the measurement of the internal electric field profile, obtained by differentiation of a measured potential distribution, it becomes possible to investigate in which part of the cell and to which extent the electric field is altered by electric bias, by illumination from outside or by degradation, for different types and qualities of solar cells. Thus, the measurement promises important information for investigating and optimizing the cell parameters by means of defect-engineering [17], i.e., to optimize the electric field profile in degraded cells in order to increase the long-time stability of the cells.

Beyond the traditional field of application to failure analysis in integrated circuits, the electron-beam tester (EBT) technique offers the possibility to measure the above internal potential distribution [6, 7, 8, 10, 13] with high spatial resolution and accuracy in determining surface potential differences if an appropriate preparation method can be developed which makes the depth dimension of the device accessible to the EBT.

Measuring Method

The measurements were carried out using the electron-beam tester ICT 9010 (Integrated Circuit Testing GmbH, Heimstetten, München, Germany); Figure 1 shows the experimental set up. The electron probe focussed to a spot diameter of 200 nm at an energy of 0.5 keV to 1 keV, which is sufficiently low to avoid charge-up effects or even damage of the semiconductor material, was scanned across a small part of the sample after it had undergone the preparation procedure described in the next section. The energy shift of the secondary electrons (SE) following the variation of the sample potential was measured with an in-lens retarding-field spectrometer by adjusting the retarding-grid voltage in such a manner that the integral SE signal stayed constant [12]. In

*Address for correspondence:

H. Schmoranzer

Department of Physics,

University of Kaiserslautern,

D-67663 Kaiserslautern, Germany

Telephone number: (49) 631-205 2329

FAX number: (49) 631-205 2394

E.mail: agschmor@rhrk.uni-kl.de

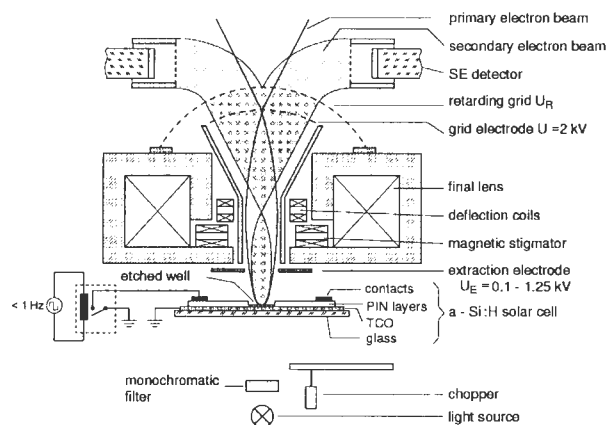


Figure 1. Experimental setup for measuring the potential difference distribution. Lower part of the EBT (ICT 9010) with supplements for *in situ* illumination and biasing of an a-Si:H solar cell. (TCO = transparent conductive oxide).

order to eliminate the effects of topography and material contrast on the number of released SE, the waveform-measurement testing mode was used. Thus, a pure potential contrast signal, free from the effects mentioned above, was obtained by difference measurement with respect to a definite reference state of the device. Obviously, only difference potentials and field profiles are measured in general in the waveform-measuring mode. However, as will be shown later, absolute electric field profile measurements could be achieved by means of a proper choice of reference state.

In contrast to an earlier work [6], the thin film solar cells were *in situ* illuminated at wavelengths $\lambda = 450$ nm, 552 nm or 650 nm and an illumination power of $33 \mu\text{W}/\text{cm}^2$, $197 \mu\text{W}/\text{cm}^2$ or $213 \mu\text{W}/\text{cm}^2$, respectively. To get another state of the solar cell, the contacts of the cell were connected or released, triggered by an external square wave voltage (open circuit / short circuit), or the illumination was chopped in the open-circuit state of the solar cell. Both types of changes of the cell state were performed at very low frequencies (< 1 Hz), because high frequency signals, as usually applied in the EBT technique, were found to be unsuitable for the solar cells. These thin film devices are only about 300 to 400 nm thick so that their high capacity prevents a rapid change of electric states. For that reason, a trigger frequency of 4 MHz was used for the tester only.

With a temperature-variable sample holder, the solar cell temperature could be changed in a wide range (100 K to 400 K). Measurements were carried out at different temperatures and also *in situ* annealing of degraded solar cells was performed, with measurements of the potential difference distribution before and after the

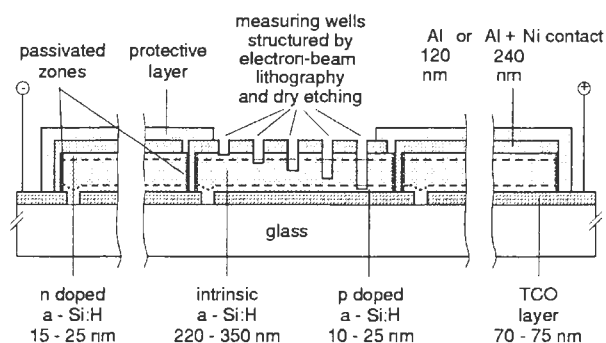


Figure 2. Schematic cross section of a p-i-n a-Si:H solar cell with etched measuring wells.

annealing by means of the special sample holder.

It is important to note that normally, for the reason mentioned above, electric surface field difference profiles, only between two specially realized states of the cell, can be measured with the EBT method. However, the absolute surface field profile can also be measured if a special reference state can be realized in the cell, e.g., by illumination or biasing, for which the potential distribution through the cell is constant or known. Then, the potential difference distribution with respect to this constant potential will yield the desired absolute potential profile of the investigated cell state and, by differentiation, the absolute field profile. To generate this constant potential profile, either illumination of very high intensity in the open-circuit state or forward biasing at high (500 mV to 800 mV for a-Si:H solar cells) voltage is needed. Whereas crystalline silicon solar cells are not affected by these conditions [10, 13], amorphous silicon cells could be easily damaged. Under high intensity illumination, the amorphous solar cells would degrade and at high bias voltages, electric break-throughs in the prepared a-Si:H layers, depending on the quality of the amorphous material, would occur. For this reason, in order to keep the amorphous silicon cells operational, a reduced illumination intensity or a reduced forward bias (400 mV) were used to realize the special reference state. However, the measurements showed that the ideal flat-band state [11] was almost attained (see Experimental Results).

Sample Preparation

For the EBT measurement of the internal potentials, the bulk depth profile of the cells had to be made accessible to EBT, i.e., transferred to a surface of the sample by a suitable preparation method. In doing so, the depth dimension of the thin cells (400 nm) has to be subdivided by the preparation into a series of many steps of varying depth so that the depth profile of the potential

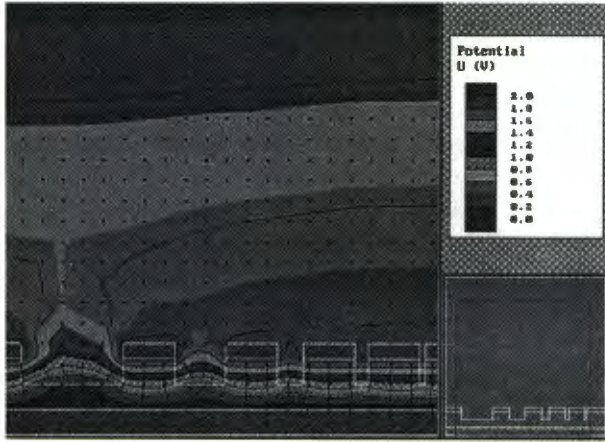


Figure 3. Simulation of the electrostatic problems connected with the preparation geometry.

can be determined with a sufficient number of measuring points in spite of the comparatively limited lateral resolution of the tester (200 nm).

In order to fulfill these requirements, the cells were coated with a thin (approximately 1 μm) plasma-resistant Novolake resist AZ PF 514 (Hoechst AG, Wiesbaden, Germany) into which a mask of holes was structured by electron-beam lithography (EBL) {Raith ELPHY I or Proxy Writer (Raith GmbH, Dortmund, Germany) in a Stereoscan 240 (Leica Cambridge Ltd., Cambridge, UK) scanning electron microscope (SEM)}. Then, cylindrical measuring wells of different depths (Fig. 2) were etched into the p-i-n a-Si:H solar cell through the holes in the resist with a low-energy quasineutral plasma beam from a HF broad-beam plasma source. Argon was used to etch through the aluminum/nickel contact and CF_4 with 25% O_2 was used to etch the amorphous silicon layers. Nevertheless, the solar cell kept perfectly working, i.e., the characteristic features of the cell like resistance and photovoltage, which are very sensitive to surface defects or changes in the bulk material, were exactly the same before and after this preparation procedure.

Reliability of the Measuring Method

The preparation process must ensure that the measured surface potential at the bottom of the wells and the wanted bulk potential profiles be correlated in a definite way. This correlation is determined essentially by three factors:

(1). On the prepared surface of the solar cell, localized surface states in the mobility gap of the a-Si:H are surely created and occupied. This newly created space charge region causes a band bending in the direction toward the semiconductor surface. There is good reason to assume that this band bending is the same all over the

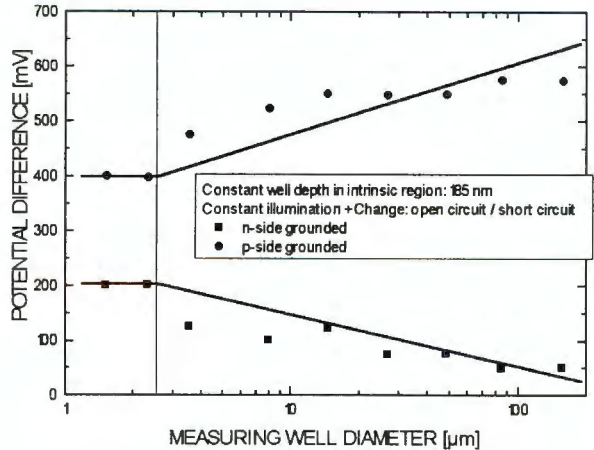


Figure 4. Measured surface potential difference in wells of the same depth but varying diameters.

prepared surface of the a-Si:H material. Thus, it represents only a constant potential shift which is eliminated by the special EBT difference-measurement method.

(2). Any other surface alterations which may be caused by the preparation process as, e.g., material mixing, implantation of defects, trenching, faceting or redeposition effects are minimized by the applied low-energy (200 eV) chemical plasma beam etching which produces volatile compounds leaving the semiconductor surface free from redeposition effects.

(3). Previous comparison measurements [7] performed on p-i-p and n-i-n structures have shown that the potential measuring results are influenced by the measuring geometry if this geometry deviates from a vertical cut through the layer system of the solar cell. On the other hand, theoretical simulations showed that the bulk potential exists uninfluenced along a vertical wall through the layer system. Therefore, the bulk potential at a certain depth can be measured at the flat bottom of a cylindrical well etched perpendicularly into the layer system. Furthermore, the smaller the diameter of the well, the less influenced is the bulk potential. This can be seen in Figure 3 which shows a plot of the simulation for this geometry, i.e., the cross-section of a solar cell with wells of various diameters but equal depths. The upper contact was biased with 2 V and the lower contact was grounded. The silicon material was assumed to be homogeneous and not illuminated, i.e., electrically passive with $\epsilon = 11.7$.

Coming up to expectations, the potential lines in the bulk material are equidistant up to the wall of the wells. In the wells, the potential lines are bent and the bottoms of the wells with large diameters do not represent equipotential surfaces. For smaller wells, however, this effect becomes negligible, i.e., potential line bending is

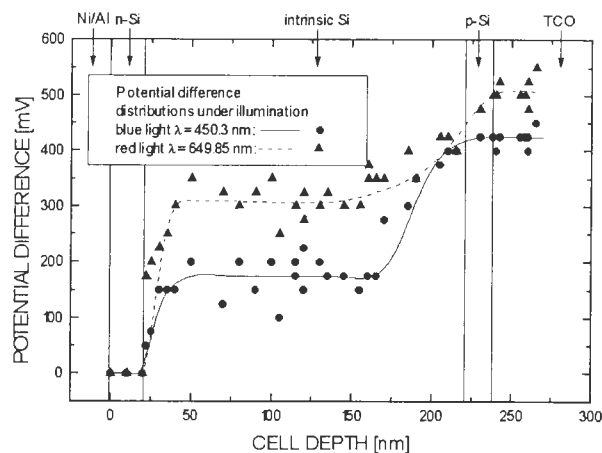


Figure 5. Measured electric potential difference distributions in an a-Si:H solar cell under illumination at different wavelengths.

negligible with respect to the resolution of the well depth measurement done by atomic force microscopy. For this reason, the lateral well dimensions should be structured as small as possible by electron-beam lithography.

On the other hand, these results of the simulation had to be verified by measurements. Therefore, wells with various diameters but equal depths were etched into the intrinsic silicon and the potential values in the bottom center of the wells were measured under illumination ($\lambda = 650$ nm, $213 \mu\text{W}/\text{cm}^2$) between the electrical states "open circuit" and "short circuit". Figure 4 shows the measuring results for wells with diameters from $1.5 \mu\text{m}$ up to $250 \mu\text{m}$. As can be seen, the measured potential values in the wells become constant for diameters smaller than $2.5 \mu\text{m}$, i.e., the deviation of the measured potential values from the true values is smaller than the noise of the SE signal (30 mV for a-Si:H; 10 mV for metals). On the other hand, the aspect ratio (ratio of the well depth to the well diameter) has to be 1 for uninfluenced EBT measurements [5]. Thus, it can be concluded that for the investigated cells of approximately $0.5 \mu\text{m}$ thickness the preparation of wells with diameters larger than $0.5 \mu\text{m}$ and smaller than $2.5 \mu\text{m}$ has no measurable influence on the potential values measured.

Experimental Results and Discussion

First of all, it was shown that in an a-Si:H solar cell in the short-circuit state under chopped illumination (all colors, see **Measuring Method**), there is no potential difference and hence no electric field difference between the states with and without illumination. This result is in agreement with theoretical predictions [3] and can easily be understood by the fact that most of the charge carriers produced by illumination are carried away via

the contacts of the solar cell. The same electric field profile is also present in the open-circuit state of the solar cell without illumination, i.e., there are three different states of a solar cell with the same electric field profile. These states were chosen as the common state in all measurements performed.

As an example, for the measured potential difference distributions, Figure 5 exhibits the ones for illumination ($\lambda = 450.3$ nm and $\lambda = 649.85$ nm) with the change between the short-circuit state and the open-circuit state. The sample was a commercial p-i-n a-Si:H indoor solar cell {Solems (Solems, Palaiseau, France) 48/32/5}. The depths of the wells were determined and related to the measuring points by means of an atomic force microscope (AFM) with very high lateral and depth resolution and an approximate error of 10 nm of the depth values (scan area $150 \times 150 \mu\text{m}^2$). Note that the different layers of the a-Si:H solar cell have been drawn in Figure 5 with their thicknesses as quoted by the manufacturer of the cell which differ from the real values measured by AFM.

Figure 6 shows the electric field difference profiles evaluated from the potential difference distributions in Figure 5. Charge carriers produced by illumination decrease the charge density distribution and hence the electric field profile. Illumination with red light affects almost only the field profile at the n-i-interface. Here, the decrease amounts to 28 mV/nm ($10 \text{ mV}/\text{nm} = 10^5 \text{ V}/\text{cm}$) whereas the decrease at the p-i-interface is 2 mV/nm only. In contrast to red light, blue light illumination leads to nearly the same decrease of about 10 mV/nm at both interfaces. A very weak decrease only was observed in the intrinsic region ($< 1 \text{ mV}/\text{nm}$) for both wavelengths. It is difficult to compare the measuring results with theoretical calculations because those calculations [3, 14] use the p- and n-layers only as constant boundary conditions despite the fact that the interface peaks of the electric field are known to be by more than one order of magnitude higher than the magnitude of the field in the intrinsic region. Consequently, in those calculations, the interface peaks are the same in different solar-cell states. In addition, all influences from outside the a-Si:H layer as, e.g., from the TCO layer or the metallic contacts have been neglected in the theoretical calculations. On the contrary, the predictions of the calculations with regard to different wavelengths of illumination were confirmed qualitatively by the measurements.

Figure 7 represents the electric field difference profile for the open-circuit state of the cell illuminated with white light of relatively high intensity ($4 \text{ mW}/\text{cm}^2$) (with respect to the common state which is open-circuit at no illumination). It can be seen that this measured profile (dashed curve) is quite similar to that profile which was

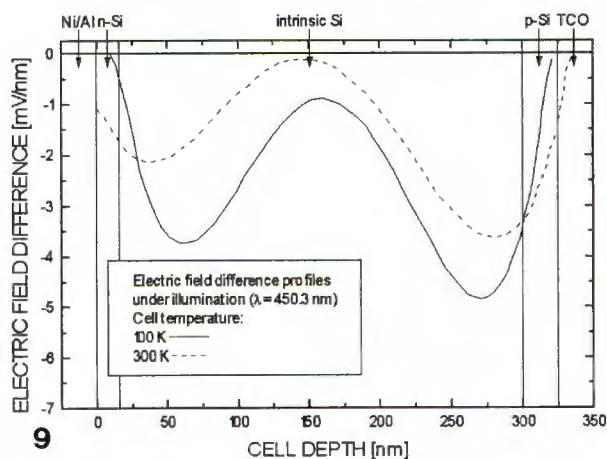
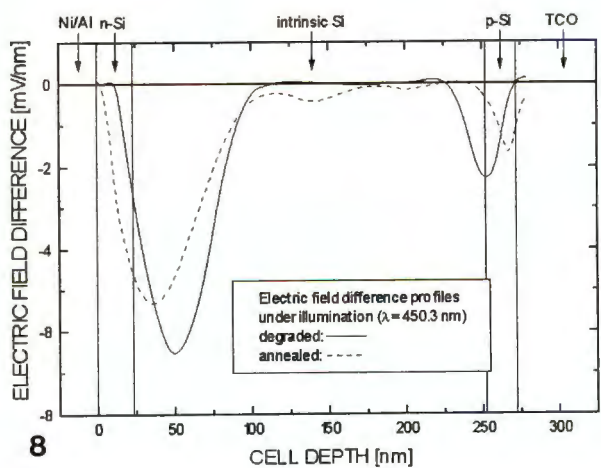
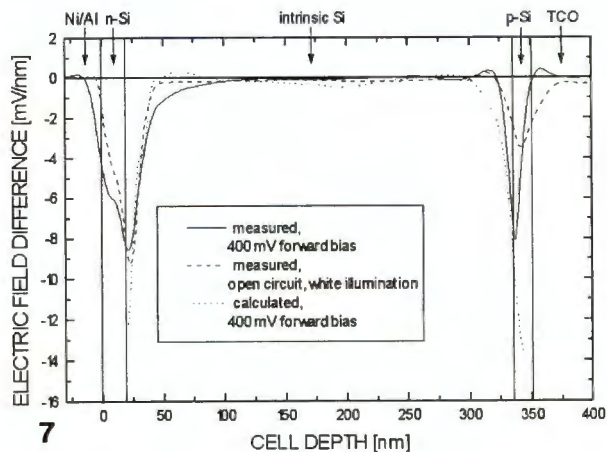
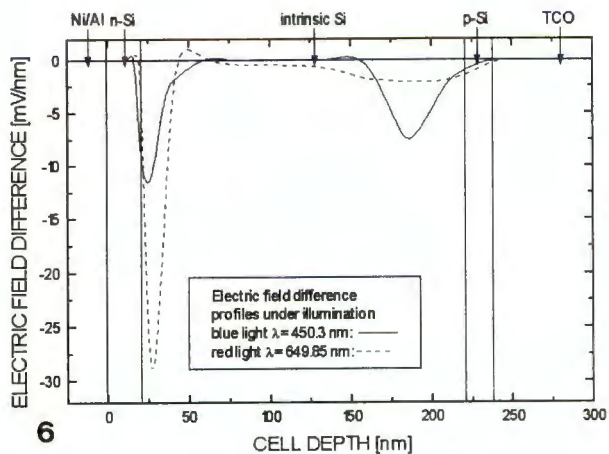


Figure 6. Electric field difference profiles in an a-Si:H solar cell under illumination of different wavelength, evaluated from the measured potential distributions (Fig. 5).

Figure 7. Comparison of different electric field profiles: measured and calculated [2] for forward bias and measured for white light illumination.

Figure 8. Electric field difference profiles in the same a-Si:H solar cell under blue illumination, degraded and annealed.

Figure 9. Electric field profiles in an a-Si:H solar cell under illumination at different cell temperatures.

measured for the state with 400 mV forward-bias voltage applied without illumination (solid curve). Although these two modes of cell operation are very different, quite similar interface peaks and a similar, very small field difference in the intrinsic region were measured.

This result can be understood as follows: by illumination, a great number of charge carriers are created in the cell which cannot leave in the open-circuit state. Thus, they reduce the internal electric field of the cell to almost zero field. The same final result is produced by the charge carriers injected by a sufficiently high for-

ward bias voltage. Obviously, both these procedures of influencing the cell state are equivalent.

In addition, the calculated electric field difference profile (calculated from the absolute profiles of [2]) for 400 mV forward bias (dotted curve) is shown in Figure 7 also. The calculated interface peaks (especially the p-i peak) are somewhat higher than the measured ones but, as this calculation was not performed for exactly the same cell parameters, the comparison is only approximate. In all, there is good agreement between the measured and the calculated profiles. Furthermore, since the

absolute potential profile for 400 mV forward bias voltage is almost constant through the cell [2], this special cell state is nearly the desired flat-band reference state. Thus, the measured field difference profiles (with respect to the common state) for 400 mV forward bias, as well as for illumination with white light at open circuit, represent almost the **absolute** field profile which exists in the cell for the common state, i.e., the short-circuit state without illumination. The similarity of the measured difference profiles (Fig. 7) shows that the flat-band state was nearly attained in both cases.

The penetration depth of photons in a-Si:H depends on their wavelength. Red light is weakly, and thus, uniformly absorbed through the layers whereas blue light is strongly absorbed. Consequently, the decrease of the electric field is stronger at the p-i-interface for blue light and at the n-i-interface for red light. In addition, electrons have a higher mobility than holes and the metallic back contact reflects the photons back into the layer system of the solar cell. This leads to a stronger decrease at the n-i-interface for all wavelengths.

Degradation in the case of a-Si:H means an increase of defect density and for that reason a change in the electric field profile [4]. In degraded solar cells, the field peaks at the interfaces are higher but the field strength values in the intrinsic region are lower than in a new cell. It follows for degraded solar cells that under illumination, the decrease of the electric field is stronger at the interfaces and weaker in the intrinsic region in comparison with a new or annealed cell. In order to degrade the solar cells for the measurements, they were illuminated for 240 h with AM 1 while cooled. The solar cells were annealed by baking them for 2 hours at 120°C. Figure 8 exhibits the electric field difference profile for the same solar cell, degraded and annealed, at open circuit with and without illumination. It can be seen that the above statement is confirmed. The shift of the interface peaks towards the intrinsic region was not explained by theoretical predictions due to the fact that, as mentioned above, the p- and n-layers represent only boundary conditions in the theoretical calculations.

The measurements on solar cells at different temperatures are shown in Figure 9. For a temperature of 100 K, the electric field difference is larger than for 300 K. This results from the fact that for lower temperatures the electric field in the solar cell becomes stronger, in qualitative agreement with theoretical calculations [1, 14] which predict that for lower temperature the open-circuit voltage and hence the electric field is higher. This measurement was carried out on a different solar cell than in the other measurements. For this particular cell, an extreme difference between the measured thickness of the a-Si:H solar cell layers and the drawn in manufacturer's specifications occurs.

Conclusion

The advantage of this EBT-EBL method obviously lies in the possibility of precise and low-energy measuring of the internal potential distribution and the internal electric field profile in semiconductor devices as, e.g., a-Si:H solar cells, for arbitrary bias [6] and illumination states controlled from outside. *In situ* degrading, annealing, heating or cooling of the sample is available, too. The possibility of arbitrary biasing and illumination of the samples during the measurements is the basic advantage of this measuring method in comparison with other methods like Auger electron spectroscopy (AES) [16], scanning probe microscopy (SPM) [15] or time-of-flight spectroscopy (TOF) [9]. Normally, potential difference distributions are measured with respect to a definite reference state. In addition, absolute potential and field profiles can be obtained, too, by means of a special reference state in the semiconductor device with a constant potential distribution.

The EBT-EBL method was applied to new, degraded and annealed a-Si:H solar cells under various illumination conditions and sample temperatures. That way, existing predictions of theoretical calculations from the literature and the assumptions underlying the models used were subjected to detailed experimental tests. For these devices, special flat-band reference states for the EBT measurements were found and the possibility to perform absolute measurements of the internal electric field was demonstrated. In addition, it can be expected that the combination of EBL micro-structuring and EBT methods will become an important diagnostic tool for defect-engineering to increase the long-time stability of the a-Si:H solar cells.

Acknowledgements

This work was supported by the German Federal Ministry of Research and Technology under contract no. 0329116 A. The authors would like to thank Prof. Dr. H. Ehrhardt for the opportunity to perform the atomic force microscopy measurements in his laboratory and Dipl.-Phys. W. Herbst for his informative discussions in the field of a-Si:H solar cells.

References

- [1] Asensi JM, Andreu J, Bertomeu J, Puiddollers J (1992) Interface effects in amorphous silicon solar cells. In: Proc. 11th E.C. Photovoltaic Solar Energy Conf. (Montreux). Guimaraes L, Palz W, De Reyff C, Kiess H, Helm P (eds.). Harwood Acad. Publ., Chur, Switzerland. pp. 769-772.
- [2] Caputo D, Irrera F, Palma F (1989) Hyperbolic

Approximation of non-uniform electric field for an analytical solution of the a-Si p-i-n structure. In: Proc. 9th E.C. Photovoltaic Solar Energy Conf. (Freiburg). Luque A, Sala G, Palz W, Dos Santos G, Helm P (eds.). Kluwer Acad. Publ., Dordrecht, Netherlands. pp. 95-98.

[3] Hack M, Shur M (1985) Physics of amorphous silicon alloy p-i-n solar cells. *J. Appl. Phys.* **58**: 997-1020.

[4] Hamakawa Y, Okamoto H (1983) Device physics and optimum design of the amorphous silicon solar cells. In: *Amorphous Semiconductor Technologies and Devices*. Hamakawa Y (ed.). Ohmsha Ltd., Tokyo. pp. 182-203.

[5] Heiland R, Leslie A (1994) Combining electron and focused ion beam techniques for failure analysis and design verification of integrated circuits. *Microelectron. Eng.* **24**: 51-58.

[6] Jank A, Jung M, Schmoranzler H (1994) Application of electron-beam testing technique to potential profile measurements in thin film semiconductor devices. *Microelectron. Eng.* **24**: 139-146.

[7] Jank A, Mayer A, Schmoranzler H (1992) Measurement of the electric field distribution in submicron semiconductor film devices by electron-beam testing. In: *Electron Microscopy 92*, Vol. II. Lopez-Galindo A, Rodriguez-Garcia MI (eds.). Universidad de Granada, Spain. pp. 197-198.

[8] Jank A, Jung M, Schmoranzler H (1994) Measurement of the electric field difference distribution in biased and illuminated a-Si:H solar cells. In: Proc. 12th E.C. Photovoltaic Solar Energy Conf. (Amsterdam), Vol. I. Hill R, Palz W, Helm P (eds.). H.S. Stephens & Associates, Bedford, U.K. pp. 81-84.

[9] Koenenkamp R, Muramatsu S, Itoh H, Matsubara S, Shimada T (1991) Electric field profile and charge collection in a-Si:H solar cells. In: Proc. 10th E.C. Photovoltaic Solar Energy Conf. (Lisbon). Luque A, Sala G, Palz W, Dos Santos G, Helm P (eds.). Kluwer Acad. Publ., Dordrecht, Netherlands. pp. 173-176.

[10] Mayer A, Jank A, Schmoranzler H (1991) Electric field in a-Si solar cells measured by electron-beam testing. In: Proc. 10th E.C. Photovoltaic Solar Energy Conf. (Lisbon). Luque A, Sala G, Palz W, Dos Santos G, Helm P (eds.). Kluwer Acad. Publ., Dordrecht, Netherlands. pp. 1095-1097.

[11] Pfeleiderer H (1991) Surface recombination in a-Si solar cells. *J. Non-Cryst. Sol.* **137&138**: 1205-1208.

[12] Plies E (1990) Secondary electron energy analyzers for electron-beam testing. *Nucl. Instr. Meth. Phys. Res.* **A298**: 142-155.

[13] Schmoranzler H, Mayer A, Jank A (1991)

Measurement of the electric potential in silicon solar cells employing an electron-beam tester. *Fresenius Z. Anal. Chem.* **341**: 251-254.

[14] Smole F, Furlan J (1992) Photoelectric properties of p-i-n a-Si:H solar cells degraded by monochromatic light of different wavelengths. In: Proc. 11th E.C. Photovoltaic Solar Energy Conf. (Montreux). Guimaraes L, Palz W, De Reyff C, Kiess H, Helm P (eds.). Harwood Acad. Publ., Chur, Switzerland. pp. 765-768.

[15] Szostak DJ, Goldstein B (1984) Photovoltage profiling of hydrogenated amorphous Si solar cells. *J. Appl. Phys.* **56**: 522-530.

[16] Waldrop JR, Harris LS (1975) Potential profiling across semiconductor junctions by Auger electron spectroscopy in the scanning electron microscope. *J. Appl. Phys.* **46**: 5214-5217.

[17] Wyrsh N, Fischer D, Shah A (1994) Determination of internal electrical field profile in a-Si:H solar cells. In: Proc. 12th E.C. Photovoltaic Solar Energy Conf. (Amsterdam), Vol. I. Hill R, Palz W, Helm P (eds.). H.S. Stephens & Associates, Bedford, U.K. pp. 73-76.

Discussion with Reviewers

M. Kittler: You prepare a series of cylindrical wells of different depth to study the depth profile of the internal electric potential/field in semiconductor devices. Would it be possible to use angular bevels too, instead of these wells?

Authors: In an early stage of the measurements, we used etched craters [13] which also have tilted walls. However, measurements on p-i-p or n-i-n layer systems showed that the surfaces of constant potential were extremely distorted by this preparation method. A linear decrease of the potential through the cell was expected but the measured potential distribution was bent. Therefore, angular bevels are expected to produce distortions, too, and should be carefully tested before use.

M. Kittler: Your method could also be applied to semiconductor devices structures made of monocrystalline Si and other semiconductor materials as well. For such devices capacity-voltage (CV) or spreading resistance (SR) measurements, for instance, are widely applied to determine the depth distribution of electrically active dopants, allowing conclusions on the depth distribution of the electric field. Please comment on the specific advantage of your technique as compared to standard methods as CV, SR etc., and did you compare your technique with well-established "standard techniques" to prove the accuracy?

Authors: There are no examples of CV or SR applications to a-Si:H solar cells in the literature. Other tech-

niques, which have been applied to solar cells, are mentioned in the conclusion: AES uses primary electrons of much too high energy. SPM which means a Kelvin probe technique requires a removal of the cell material during measurement. The TOF method leaves out the inner intrinsic region whereas our method determines the complete field profile. Comparisons with "standard techniques", applied to a-Si:H cells of different dimensions, yielded qualitative agreement. A specific advantage of our method lies in the possibility of carrying out non-destructive measurements under arbitrary illumination and biasing.

M. Kittler: Extended defects (e.g., grain boundaries or dislocations) in semiconductors are often charged and consequently, connected with a space charge / band bending. Would it be possible to study the electric field distribution around such defects by your technique?

Authors: In combination with a measuring method that gives the absolute three-dimensional position of the defect and a little fine tuning of our etching process, one can expect that such studies would be possible.

H. Niedrig: What is the principle of the waveform-measurement testing mode? Can you give references for further reading?

Authors: The waveform mode is used to measure the potential changes on a specific spot of the specimen caused, e.g., by an external biasing. To do this, the secondary electron signal is measured at alternating bias. If the secondary electron distribution is shifted along the energy axis caused by the potential change of the specimen, the voltage of the retarding grid U_R (see Fig. 1) is altered accordingly so that the distribution is shifted back to its original position on the energy axis. The difference of the voltages applied to the retarding grid is equal to the potential difference on the specimen. For further reading, see additional references [18, 19].

E. Plies: You mention that a beam voltage of 0.5 kV to 1 kV is sufficiently low to avoid charge-up effects. But in electron-beam testing, there is also an influence of the extraction field on the charge-up effect. What value for the extraction voltage U_E at the extraction electrode in Figure 1 is used for your measurements?

Authors: The extraction voltage U_E we used was 1 kV or 1.2 kV.

E. Plies: The measured potential difference distributions in Figure 5 are not very smooth. How are the electric field difference profiles of Figure 6 evaluated from these measured distributions, i.e., which curve fitting or smoothing techniques are used before (and after) differentiation? Could you comment on the overswings

of the field difference profiles?

Authors: Since there is no analytical fit function for the potential distribution, we used a special kind of splines which do not necessarily go through the measuring points in Figure 5. The field profiles in Figure 6 were evaluated from these splines (in Fig. 5) by differentiation. The overswings are artifacts from the numerical fitting and could not be completely avoided.

L.J. Balk: Can you explain in more detail why frequencies of more than 1 Hz are unsuitable for solar cells? It seems that this might be overcome by, for instance, using low measuring impedances.

Authors: It is possible to modulate the electric bias or chop the illumination of the a-Si:H solar cells with higher frequencies up to some kHz, but square-wave voltages with usual EBT frequencies (MHz) were extremely distorted when applied to the thin film cells. The main reason to use such low frequencies was that the measuring procedure was not fully automated and it was more convenient for the operator to deal with frequencies below 1 Hz.

L.J. Balk: You discuss the influence of the well diameter on the achieved preciseness. How is the well depth affecting it, say, by changed trajectories of the electron?

Authors: The important parameter of the measuring well is the aspect ratio (ratio of the well depth to the well diameter) which influences the trajectories of the electrons because the potential surface at the bottom of the well are bent more or less (depending on that ratio) upwards (see Fig. 3).

Additional References

[18] Fuchs E, Oppolzer H, Rehme H (1990) Particle Beam Microanalysis: Fundamentals, Methods and Applications. VCH Verlagsgesellschaft mbH, Weinheim, Germany. Chapter 8.

[19] Herrmann KD (1989) Verbesserung der Testbarkeit höchstintegrierter Schaltkreise durch einen Elektronenstrahlprüffreundlichen Schaltungsentwurf (Improvement of the testability of highly integrated circuits by a circuit design appropriate to electron-beam testing). Duisburger Mikroelektronik, Band 3. Verlagsbuchhandlung Nellissen-Wolff, Aachen. Germany. Chapter 2.